Japanese Journal of Applied Physics
Vol. 47, No. 3, 2008, pp. 1871–1875

Recrystallization Behavior of Silicon Implanted with Phosphorus Atoms by Infrared Semiconductor Laser Annealing

Toshiyuki SAMESHIMA*, Yasuhiro MATSUDA[1], Yasunori ANDOH[1], and Naoki SANO[2]

Tokyo University of Agriculture and Technology, Koganei, Tokyo 184-8588, Japan
[1]*Nissin Ion Equipment Co., Ltd., Koka, Shiga 528-0068, Japan*
[2]*Hightec Systems Corporation, Yokohama 222-0033, Japan*

(Received July 11, 2007; accepted October 16, 2007; published online March 21, 2008)

We report the recrystallization behavior of silicon implanted with phosphorus atoms at 10 and 70 keV with a dose of 2×10^{15} cm^{-2}. The samples were coated with a 200-nm-thick diamond-like-carbon optical absorption layer and then annealed by irradiation with a 940 nm continuous-wave laser at 70 kW/cm^2. An analysis of optical reflectivity spectra showed an in-depth distribution of the crystalline volume ratio. The amorphized surface regions produced by the phosphorus implantation were recrystallized from the bottom region by laser annealing. They were almost completely recrystallized by the laser annealing for 2.6 ms. The in-depth profiles of phosphorus concentration hardly changed for the laser annealing for 2.6 ms. The implanted regions were effectively activated by the laser annealing and the sheet resistance markedly decreased to 102 and 46 Ω/sq for implantion at 10 and 70 keV, respectively. [DOI: 10.1143/JJAP.47.1871]

KEYWORDS: activation, dopant, crystallization, reflectivity, crystalline-volume ratio

1. Introduction

Rapid heating is important in order to activate semiconductor materials implanted with impurity atoms.[1,2] A high activation ratio and no serious impurity diffusion are required to fabricate transistor devices with a short channel. We have recently proposed an annealing method on the order of 10^{-5} to 10^{-3} s using infrared lasers.[3–5] An infrared laser is an attractive light source because stable lasers with a high power of ~10 kW and a high efficiency of ~50% have been developed. We use a carbon optical absorption layer in order to solve the problem of the low optical absorbance of silicon in infrared regions. A black carbon layer with a high heat resistivity of ~5000 K can serve as a heat source at high temperatures. Silicon is effectively heated by heat diffusion from the adjacently placed carbon layer.[6]

In this paper, we propose an evaluation of the crystalline properties for the surface regions implanted with phosphorus atoms by analyzing optical reflectivity spectra. We report the recrystallization behavior of disordered amorphous regions formed by implantation using infrared laser annealing. We also report that initial phosphorus in-depth profiles are not significantly changed by laser annealing. We demonstrate an effective activation and a low electrical resistance.

2. Experimental Procedure

The ion implantation of phosphorus atoms was conducted for p-type silicon substrates with a resistivity of 10 Ω cm. The acceleration energies were 10 and 70 keV. The dose was 2×10^{15} cm^{-2}. Graphitic diamond-like carbon (DLC) films with a thickness of 200 nm were formed on the silicon surface by the unbalanced magnetron sputtering (UBMS) with Ar gas at room temperature at a radio frequency power of 30 W.[7] The deposition rate of the DLC film was 17 nm/min. Optical measurements revealed that the carbon layer had an optical absorbance of 70% at 940 nm, which was the wavelength of our laser light. An equipment for laser irradiation was constructed using a beam scanning mechanism. Samples were normally irradiated with a fiber-coupled continuous-wave (CW) laser diode with a wavelength of 940 nm and a power of 20 W in air at room temperature. The diameter of the core and the numerical aperture (NA) of the fiber were 400 μm and 0.22, respectively. The diverged beam was concentrated on the surface of samples by a combination of six aspherical lenses for 2 : 1 image formation. The power distribution of the beam was Gaussian like. The size of the beam spot was 180 μm at the full width at half maximum (FWHM) of the laser power distribution. The peak power density was 70 kW/cm^2 on the sample surface. Samples were mounted on an two dimensional movable stage driven by linear motors at a velocity from 3 to 20 cm/s in the Y direction. The effective laser dwell time was given by the effective beam size of 180 μm divided by the laser beam scanning velocity. The effective dwell time of the laser light ranged from 0.9 to 6.0 ms on the sample surface. The stage was also moved with a 50 μm step in the X direction. After laser irradiation, the carbon layer was removed by oxygen plasma treatment at 50 W of a 13.56 MHz radio frequency and 5×10^{-2} Pa for 20 min. Numerical heat flow simulation was carried out to estimate temperature increase at the silicon surface using a finite element heat flow program.[8]

Optical reflectivity spectra were measured between 250 and 800 nm using a conventional spectrometer. The optical reflectivity spectra were analyzed using a numerical calculation program, which was constructed with the optical interference effect for a structure of air/seven Si layers/Si-substrate.[9] The optical reflectivity at the sample surface depends on the complex refractive indexes of Si. Using the effective dielectric model, the complex refractive index $\tilde{n}_f$ with a crystalline volume ratio, X, is determined by combing the crystalline refractive index $\tilde{n}_c$[10] with the amorphous refractive index $\tilde{n}_a$[10] as,

$$\tilde{n}_f = X\tilde{n}_c + (1 - X)\tilde{n}_a \quad (1)$$

The values of the parameters of thickness and the crystalline volume ratio were changed for each of the seven doped layers to calculate the reflectivity. Figure 1(a) shows the optical reflectivity spectra calculated by the model described above when an amorphous layer with different thicknesses is

*E-mail address: tsamesim@cc.tuat.ac.jp

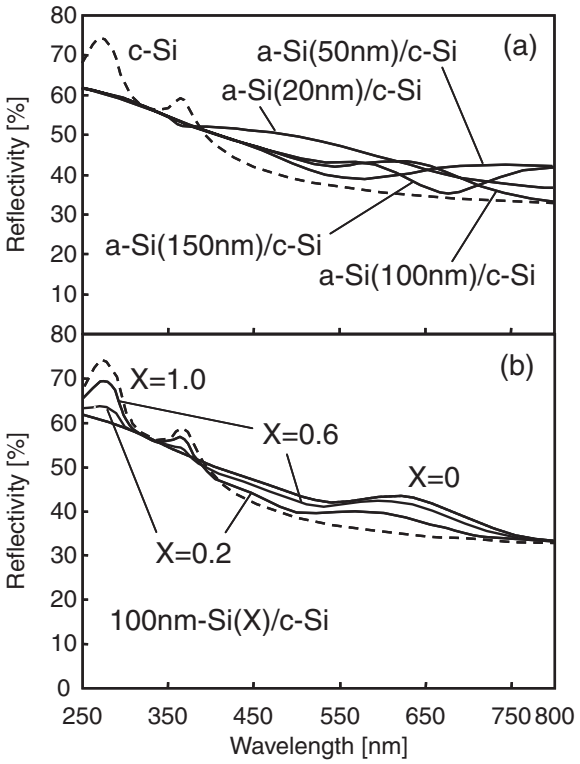

Fig. 1. Optical reflectivity spectra calculated when amorphous layer with different thicknesses is coated on surface of c-Si (a) and optical reflectivity spectra when 100-nm-thick silicon layer with different crystalline volume ratios is coated on surface of crystalline silicon (b).

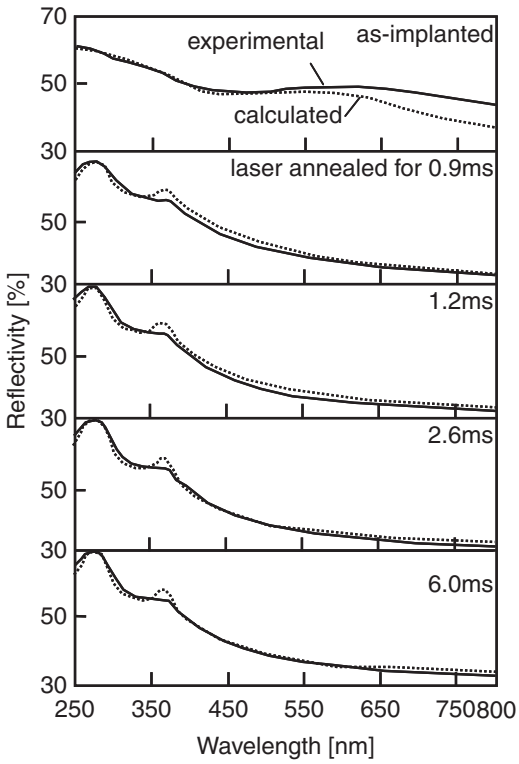

Fig. 2. Optical reflectivity spectra for samples containing 2×10^{15} cm^{-2} phosphorus as-implanted at 10 keV and laser annealed for effective dwell times of 0.9, 1.2, 2.6, and 6.0 ms, respectively. The calculated spectra are also presented (dashed curves).

coated on the surface of crystalline silicon (c-Si). The E_1 and E_2 peaks around 280 and 370 nm for c-Si disappeared when an only 20-nm-thick amorphous silicon (a-Si) layer was placed on the silicon surface because the c-Si layer was covered owing to the high absorption coefficient in the ultraviolet region.[11] On the other hand, the sample with a 20-nm-thick a-Si/c-Si layer had a strange line shape in optical reflectivity compared with the bulk c-Si from 400 to 800 nm. This resulted from the optical interference effect caused by the different complex refractive indexes between a-Si and c-Si and the low absorption coefficient. Different film thicknesses resulted in different optical reflectivity spectra between 400 and 800 nm because of a change in the optical interference effect. A thick a-Si of 150 nm caused oscillated spectra between 400 and 800 nm because of the periodic optical interference. Figure 1(b) shows the optical reflectivity spectra when a 100-nm-thick silicon layer with different crystalline volume ratios was coated on the surface of c-Si. E_1 and E_2 peaks decreased in reflectivity as the crystalline volume ratio decreased. The spectral line shape between 400 and 800 nm became different as the crystalline volume ratio decreased. These changes in the reflectivity spectra result from that the optical interference effect increased because of different complex refractive indexes with a low crystalline volume ratio compared with that of c-Si. The result of Fig. 1 indicates that optical reflectivity spectra in ultraviolet, visible, and infrared regions provide information on the crystalline volume ratio near surface regions. The most possible in-depth distribution of the crystalline volume ratio was obtained by fitting calculated reflectivity spectra to the experimental reflectivity spectra. The in-depth phosphorus concentration profiles were measured by secondary ion mass spectroscopy (SIMS). The sheet resistance was also investigated using the four-point-probe measurement system.

3. Results and Discussion

Figure 2 shows optical reflectivity spectra for samples as-implanted at 10 keV and laser annealed for effective dwell times of 0.9, 1.2, 2.6, and 6.0 ms. The optical reflectivity for the as-implanted sample showed a broad spectrum. There was no E_1 or E_2 peak in the ultraviolet region. These results indicate that the surface region was completely amorphized by the phosphorus implantation. For laser-annealed samples, the E_1 and E_2 peaks appeared at approximately 370 and 280 nm, respectively. These results indicate that the surface region was recrystallized by laser annealing. Those peaks became large as the effective dwell time of laser light increased. Figure 2 also shows the spectra calculated with the model described above. Although we believe that the calculated spectra agreed well with experimental spectra, there were small differences particularly in the ultraviolet region for laser-annealed samples. We think that the doping with a high concentration of phosphorus atoms caused a change in the complex refractive index of c-Si[12] because the 10 keV low energy implantation concentrated phosphorus atoms in the shallow surface region. The complex refractive index of the c-Si of the phosphorus-doped region was probably different from that of c-Si, used as the database for calculation.

Figure 3 shows optical reflectivity spectra for samples as-implanted at 70 keV and laser annealed for effective dwell

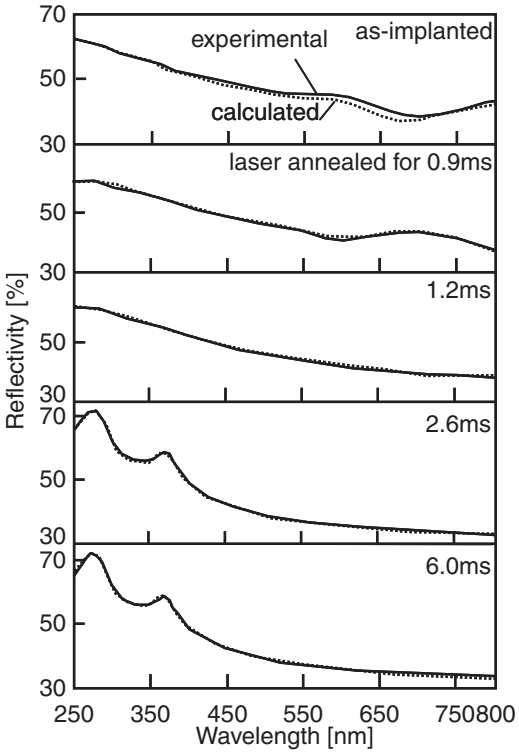

Fig. 3. Optical reflectivity spectra for samples containing $2 \times 10^{15}\,cm^{-2}$ phosphorus as-implanted at 70 keV and laser annealed for effective dwell times of 0.9, 1.2, 2.6, and 6.0 ms, respectively. The calculated spectra are also presented (dashed curves).

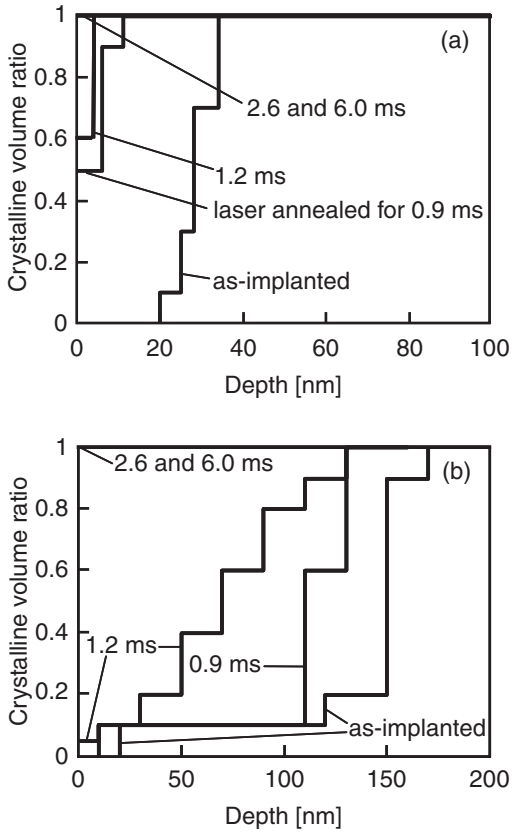

Fig. 4. In-depth distribution of crystalline volume ratio for samples as-implanted with phosphorus at concentration of $2 \times 10^{15}\,cm^{-2}$ and samples laser annealed with different laser dwell times obtained from the fitting process shown in Figs. 2 and 3 for implantation energies of 10 (a) and 70 keV (b).

times of 0.9, 1.2, 2.6, and 6.0 ms, respectively. The figure also presents calculated spectra best fit to the experimental spectra. No peak in the ultraviolet region indicates the amorphization of the surface region. An oscillation in the reflectivity spectrum was observed in the spectrum as-implanted between 500 and 800 nm. This oscillation results from a substantial optical interference effect for the air/thick amorphized region/c-Si structure. The oscillation disappeared when the effective dwell time was above 1.2 ms, although the surface was still in the amorphous state because no E_1 or E_2 peak was observed. The oscillation in the reflectivity spectra was eliminated when the complex refractive index gradually changed from the top surface into deep regions. This means that the crystalline volume ratio gradually increased from 0 to 1 as the depth increased. The E_1 and E_2 peaks appeared at approximately 370 and 280 nm for laser annealing longer than 2.6 ms. The surface region was recrystallized.

Figure 4 shows the in-depth distribution of the crystalline volume ratio for implantation at 10 (a) and 70 keV (b) with different laser dwell times obtained from the fitting process shown in Figs. 2 and 3. For phosphorus implantation at 10 keV, the 20-nm-deep region with respect to the surface was completely amorphized. There was a partially amophized region from 20 to 35 nm depths from the surface. In the initial amorphous region, the crystalline volume ratio increased to 1.0 in the deep region owing to laser annealing for 0.9 and 1.2 ms. The top 10 nm region had a mixed state of crystalline and amorphous regions. Laser annealing for 2.6 and 6.0 ms completely crystallized the implanted region, as shown in Fig. 4(a). For phosphorus implantation at 70 keV, the 20 nm deep region with respect to the surface was completely amorphized. There was a substantial amorphized region to a 150 nm depth from the surface. Laser annealing recrystallized the implanted region and the crystalline volume ratio increased from the deep region. For laser annealing for 1.2 ms, the implanted region deeper than 120 nm was almost completely recrystallized and the top 120 nm surface region had a crystalline volume ratio that gradually changed from 0 to 1 with increasing depth from the surface. For effective dwell times above 2.6 ms, the implanted region was completely recrystallized.

The heat flow calculation estimated that the surface was heated to 1150 °C by laser irradiation for 0.9 ms. It also estimated that the temperature at the surface was increased to 1220 and 1390 °C by laser irradiation for 1.2 and 2.6 ms, respectively. The heat flow calculation indicates that recrystallization in the deep implanted region occurred in the solid phase as a result of heating to a temperature higher than 1100 °C for both implantation conditions of 10 and 70 keV. On the other hand, a temperature higher than 1200 °C was necessary to complete the crystallization of the surface region. The present analysis of optical reflectivity spectra and the heat flow calculation gave interesting information, namely, the $2 \times 10^{15}\,cm^{-2}$-phosphorus-implanted region was completely crystallized in the solid phase by laser annealing for a dwell time of 2.6 ms at $70\,kW/cm^2$. The temperature increased to 1390 °C just below the melting threshold. The heat flow calculation

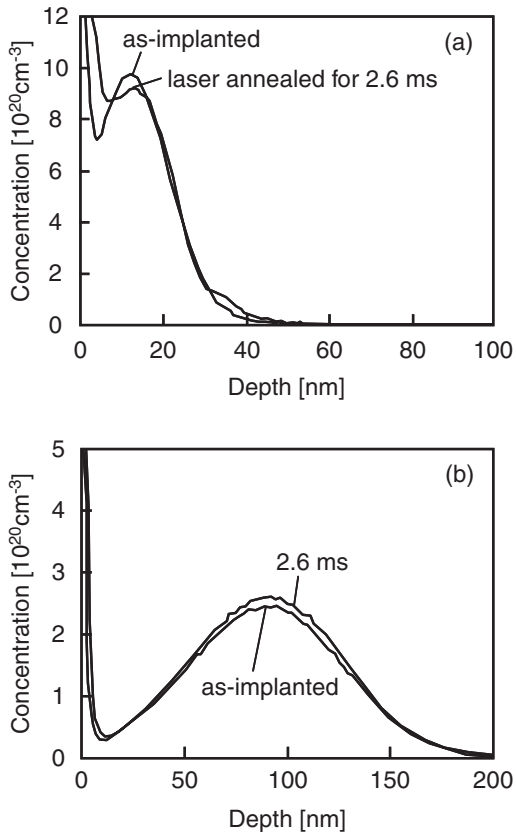

Fig. 5. In-depth phosphorus concentration profiles for samples as-implanted with phosphorus at concentration of $2 \times 10^{15}\,\mathrm{cm}^{-2}$ and samples laser annealed for effective dwell time of 2.6 ms for implantation energies of 10 (a) and 70 keV (b).

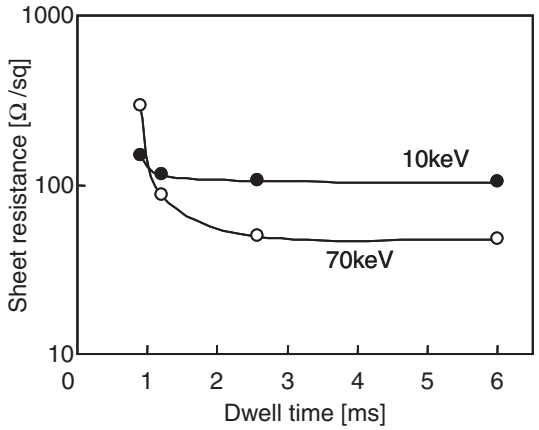

Fig. 6. Sheet resistance as a function of effective dwell time of laser irradiation for samples phosphorus implanted at 10 and 70 keV with phosphorus at concentration of $2 \times 10^{15}\,\mathrm{cm}^{-2}$.

estimated that the duration in which the temperature was above 1300 °C was about 1.5 ms for 2.6 ms laser annealing. The recrystallization rate was therefore at least 1×10^{-4} m/s (~150 nm/1.5 ms) for 70 keV implantation. Although the present recrystallization rate is much lower than that in the case of pulsed laser melt regrowth (~1 m/s), it is much higher than that in the case of solid-phase crystallization at approximately 600 °C (~1 nm/s).

Figure 5 shows the in-depth phosphorus concentration profiles for samples $2 \times 10^{15}\,\mathrm{cm}^{-2}$-as-implanted at 10 keV and samples laser annealed with an effective dwell time of 2.6 ms (a), and samples as-implanted at 70 keV and samples laser annealed with an effective dwell time of 2.6 ms (b). The phosphorus atoms were located in the surface region and the depth of the peak phosphorus concentration was 13.7 nm for as-implanted samples at 10 keV. The phosphorus implantation made the silicon surface region disordered, as shown by the in-depth profiles of the crystalline volume ratio, as shown in Fig. 4. After laser annealing, the depth of the peak-phosphorus-concentration region was 14.9 nm. Although the peak concentration slightly decreased from 9.8×10^{20} to $9.1 \times 10^{20}\,\mathrm{cm}^{-3}$, the phosphorus concentration profile hardly changed, as shown in Fig. 5(a). The results of Figs. 4 and 5 show that the phosphorus-implanted region was completely recrystallized while keeping the initial dopant concentration profiles using the present annealing method. For implantation at 70 keV, the peak phosphorus concentration appeared at 90 nm for as-implanted samples. The phosphorus atoms were deeply distributed compared with those in the case of the implantation at 10 keV. After laser annealing, the phosphorus concentration profile hardly changed. The present method achieved recrystallization in the deep region while keeping the initial dopant concentration profiles. The heat flow calculation estimated a duration of about 1.5 ms for temperatures above 1300 °C. The diffusion coefficient of phosphorus atoms in the solid silicon layer was about $1 \times 10^{-11}\,\mathrm{cm}^2/\mathrm{s}$ at a very high temperature of approximately 1300 °C.[13] The heating duration gives a diffusion length of 2.5 nm ($\sim 2\sqrt{1 \times 10^{-11} \times 1.5 \times 10^{-3}}$), which is near our maximum diffusion length determined by SIMS, as shown in Fig. 5. Millisecond-duration heat treatment will be important to activate the implanted region while keeping initial dopant concentration profiles.

Figure 6 shows sheet resistance as a function of the effective dwell time of laser light for phosphorus implantation at 10 and 70 keV and at $2 \times 10^{15}\,\mathrm{cm}^{-2}$. The sheet resistance was reduced to 148 Ω/sq by laser annealing for 0.9 ms for the sample implanted at 10 keV, while the sample implanted at 70 keV had a high sheet resistance of 288 Ω/sq after laser annealing for 0.9 ms. The low resistance for the sample implanted at 10 keV probably resulted from the effective recrystallization induced by laser annealing for 0.9 ms, as shown in Fig. 4(a). On the other hand, most of the implanted region kept the initial disordered state for the sample implanted at 70 keV as shown in Fig. 4(b). The sheet resistance decreased to 46 Ω/sq for samples implanted at 70 keV as the dwell time of laser light increased to 2.6 ms according to the recrystallization of the implanted region. However, it decreased to 106 Ω/sq for the samples implanted at 10 keV in spite of the complete recrystalization induced by laser annealing. The high sheet resistance in the case of 10 keV probably resulted from a low carrier mobility due to a high degree of impurity scattering caused by phosphorus atoms with an almost $10^{21}\,\mathrm{cm}^{-3}$ concentration near the surface region, as shown in Fig. 5(a). The results of Figs. 2–6 demonstrate that phosphorus-implanted regions were well recrystallized and that phosphorus atoms were effectively activated at a laser dwell time of 2.6 ms.

4. Conclusions

The crystalline properties in ion-implanted silicon surface

regions were analyzed using the optical interference method. Optical reflectivity spectra were calculated with a seven-layered structure formed on c-Si. Each layer had a crystalline volume ratio determined by the effective dielectric model. The calculated reflectivity spectra were fitted to experimental spectra. The fitting process gave an in-depth distribution of the crystalline volume ratio. Phosphorus atoms were implanted in a p-type silicon substrate at 10 and 70 keV at a concentration of $2 \times 10^{15}\,\mathrm{cm}^{-2}$. CW laser annealing at 940 nm and a power intensity of $70\,\mathrm{kW/cm}^2$ was applied to heat treat the samples using a 200-nm-thick DLC optical absorption layer. The optical reflectivity spectra of the silicon surface changed with the laser annealing duration. The silicon surface regions were amorphized by the phosphorus implantation. The implanted regions were crystallized from the deep region by laser annealing. When the dwell time of the laser beam was 2.6 ms, the amorphized implanted regions were almost completely recrystallized. The heat flow calculation indicates that crystallization was achieved in the solid phase during heating to a high temperature of 1390 °C. The crystallization velocity was estimated to be $1 \times 10^{-4}\,\mathrm{m/s}$ for the samples undergoing 70 keV implantation. SIMS revealed that the present laser annealing at $70\,\mathrm{kW/cm}^2$ for a dwell time of 2.6 ms hardly changed the initial phosphorus concentration of in-depth profiles. Sheet resistance markedly decreased to 102 and $46\,\Omega/\mathrm{sq}$ for $2 \times 10^{15}\,\mathrm{cm}^{-2}$ implantation at 10 and 70 keV after laser annealing, respectively. Millisecond-duration heat treatment has the potential to activate the implanted region whlie keeping initial dopant concentration profiles.

1) M. Mehrotra, J. C. Hu, and M. Rodder: IEDM Tech. Dig., 1999, p. 419.
2) K. Goto, T. Yamamoto, T. Kubo, M. Kase, Y. Wang, T. Lin, S. Talwar, and T. Sugii: IEDM Tech. Dig., 1999, p. 931.
3) T. Sameshima and N. Andoh: Jpn. J. Appl. Phys. **44** (2005) 7305.
4) T. Sameshima, M. Maki, M. Takiuchi, N. Andoh, N. Sano, Y. Matsuda, and Y. Andoh: Jpn. J. Appl. Phys. **46** (2007) 6474.
5) N. Sano, M. Maki, N. Andoh, T. Sameshima, Y. Matsuda, and Y. Andoh: Jpn. J. Appl. Phys. **46** (2007) L620.
6) T. Sameshima and N. Andoh: Mater. Res. Soc. Symp. Proc. **849** (2004) KK9.5.
7) S. Yamg, D. Camino, A. H. S. Jones, and D. G. Teer: Surf. Coat. Technol. **124** (2000) 110.
8) R. W. Lewis: *Fundamentals of the Finite Element Method for Heat and Fluid Flow* (Wiley, NewYork, 2004) Chaps. 3–5.
9) M. Born and E. Wolf: *Principles of Optics* (Pergamon, New York, 1974) Chaps. 1 and 13.
10) E. D. Palik: *Handbook of Optical Constants of Solids* (Academic Press, NewYork, 1985) pp. 562 and 577.
11) J. R. Chelikowsky and M. L. Cohen: Phys. Rev. B **10** (1974) 5095.
12) L. Vina and M. Cardona: Phys. Rev. B **29** (1984) 6739.
13) A. S. Grove: *Physics and Technology of Semiconductor Devices* (Wiley, New York, 1967) Chap. 3.